Plasma Medicine, 6(2): 179–191 (2016)

A Microsecond-Pulsed Cold Plasma Jet for Medical Application

Chao Zheng,[a] Yanqin Kou,[a] Zhen Liu,[b,*] Anna Zhu,[c] Hongqiang Jiang,[a] Yifan Huang,[b] & Keping Yan[b]

[a]Zhejiang Center for Medical Device Adverse Event Monitoring and Safety Research, Hangzhou 310009, China; [b]Institute of Industrial Ecology and Environment, Collage of Chemical and Biological Engineering, Zhejiang University, Hangzhou 310028, China; [c]State Key Laboratory of NBC Protection for Civilian, Beijing 102205, China

*Address all correspondence to: Zhen Liu, Institute of Industrial Ecology and Environment, Collage of Chemical and Biological Engineering, Zhejiang University, Hangzhou 310028, China; Tel.:+86-571-88273897; Fax: +86-571-88210786, E-mail: zliu@zju.edu.cn

ABSTRACT: A homemade cold plasma jet device for medical application is introduced here. It consists of a microsecond-pulsed power source and a handheld jet gun. The pulse width is 1.2 μs, and the average plasma power is <10 W. Both helium (He) and argon (Ar) gas were used to generate touchable cold plasma jet, and the maximum jet lengths were 7 cm and 3 cm, respectively. Pulsed voltage and gas flow have significant influence on jet formation. The emission spectra of the He and Ar jets were compared. When *Staphylococcus aureus* was treated on a 90-mm agar plate for 0.5–2.5 min, bactericidal spots of 0.5–5.0 cm were obtained. In terms of disinfection of *Staphylococcus aureus* on a 10-mm quartz plate, Ar plasma performs more efficiently than He plasma.

KEY WORDS: non-thermal plasma**,** plasma jet, plasma medicine, pulsed power, disinfection

I. INTRODUCTION

In recent decades, plasma medicine has shown great potential in many clinical aspects such as skin disinfection,[1] wound healing,[2] blood coagulation,[3] cancer therapy,[4] dentistry,[5] dermatology[6] and plastic aesthetic surgery.[7] Up to now, numerous reports have confirmed the effectiveness of clinical plasma medicine through *in vitro/in vivo,* animals and human trial studies.[8–11] Clinical plasma medicine has advantages over existing traditional medical technologies in certain applications, for instance, severe burns or chronic wounds. To fully understand the mechanism of plasma medicine, many studies have focused on the interactions of plasma and living tissues, reactive oxygen and nitrogen species (RONS) and oxidative stress, and immune responses.[12–15] Plasma medicine may become a powerful tool for disease control in the future.

Plasma jet and dielectric barrier discharge (DBD) plasma are the most popular devices used in plasma medicine. Plasma devices are critical for medical applications, and they need certification from the FDA or other government agency before their commercialization. Until now, only a few integrated plasma medical devices have been reported, and very few have obtained approval from government agencies. Rhytec Portrait® PSR3 is the first commercialized plasma jet medical device for plastic and aesthetic surgery

to obtain approval from U.S. FDA in 2007.[16] The plasma torch MicroPlaSter® has performed well during many clinical trials for wound and ulcer healing since 2008.[17] The plasma jet kINPen® developed by INP (Leibniz Institute for Plasma Science and Technology, Germany) has been used in many clinical studies, and recently received German certification as medical device class IIa.[18] The AlmaPlasma Company in Italy developed a plasma gun for dentistry that employs a compressed gas tank to supply argon (Ar) gas for 30-min treatments.[19] Lu et al. also developed a prototype of plasma device for root canal treatment, and the device is currently under clinic trial.[20] Other typical prototypes for medical applications include a plasma dispenser,[21] a portable plasma flashlight,[22,23] and a plasma endoscope.[24]

In this paper, we present our recently developed pulsed-plasma jet device. A specially designed microsecond-pulsed power supply and a handheld plasma gun have been integrated as a medical device. The jet is touchable and cold and can be applied in clinical medicine. We present the physical characteristics of jet and the preliminary biological disinfection results.

II. EXPERIMENTS AND METHODS

A. Pulsed Plasma Jet Device

Figure 1 shows our home-made integrated plasma jet device. It consists of a microsecond-pulsed power source and a handheld jet gun. The diameter of jet gun is ~25 mm. The pulsed-power source can produce high-voltage pulses with a peak value up to 12 kV, a pulse width of 1–2 μs, and a repetition rate up to 30 kHz (i.e., kpps, kilopulses per second). Cylinder gas is used for the present setup. Either helium (He) or Ar gas can be used for plasma jet generation, and the gas flow rate can be adjusted by a flow meter in the panel within 2–10 L/min. Figure 2 shows the schematic diagram of the jet gun. Two quartz tubes are used as an insulating medium and to generate a double-dielectric bar-

FIG. 1: Pulsed cold plasma jet device with a handheld jet gun.

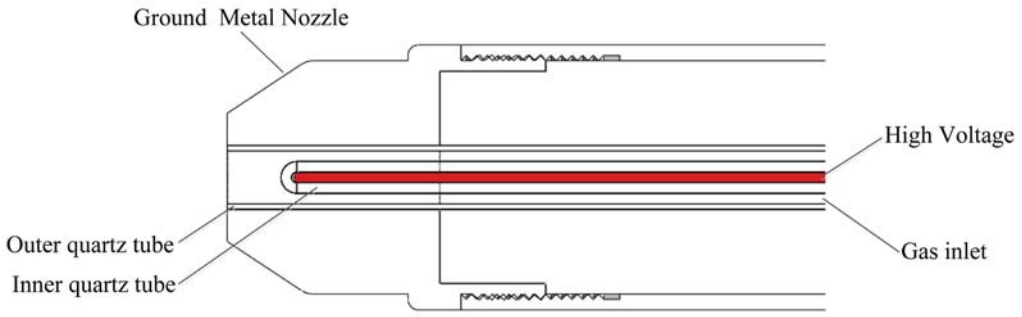

FIG. 2: Schematic diagram of jet gun.

rier discharge (DDBD) plasma. The high-voltage electrode is located in the axis and is encased by the inner quartz tube. The outer quartz tube with inner diameter of 4 mm is placed around a grounded metal nozzle; thus, discharge between the two quartz tubes is 0.5 mm. A touchable cold plasma jet can be produced from the nozzle with a diameter of ~4 mm. This plasma gun can be held in the human hand and can be conveniently operated in certain areas through the flexible metal tube. When He gas was used, a 7-cm-long jet was obtained (Fig. 1). Compared with other reported plasma jets,[18, 19] this plasma device can produce a longer plasma jet.

B. Measurement Methods

All electrical measurements were conducted using an oscilloscope (Tektronix MDO 3024), a high-voltage probe (Tektronix P6015A), and a current probe (Tektronix TCP0030A). Photos of the plasma jet were taken with a digital camera (Nikon D7000). A multichannel fiber optical spectrometer (Avantes AvaSpec-2048-8-USB2) was used for the emission spectrum of plasma jet, and element analysis software (PLASUS SpecLine, version 2.1) was applied to analyze the species of plasma.

C. Plasma Surface Disinfection

As shown in Fig. 3, bacteria *Staphylococcus aureus* ATCC6538 were selected to evaluate disinfection efficiency of the jet qualitatively and quantitatively on an agar plate (Φ 90 mm) and a quartz plate (Φ 10 mm). The bacteria were first cultivated for 8–10 hours at 37°C in a prepared nutrient broth to a cell density of ~10^9–10^{10} CFU/mL. Bacteria were then sprayed onto an agar plate using a special spray bottle in biosafety cabinets or coated on a quartz plate with properly diluted bacteria suspension. After plasma treatment (Fig. 3), the heterotrophic plate count (HPC) method was used to detect survival bacteria. The plasma-treated agar plates were directly transferred to a 37°C incubator and stored for 12–24 hours, and the diameter of bactericidal spots were then measured. Bacteria on a quartz plate were first washed with 2 mL sterilized

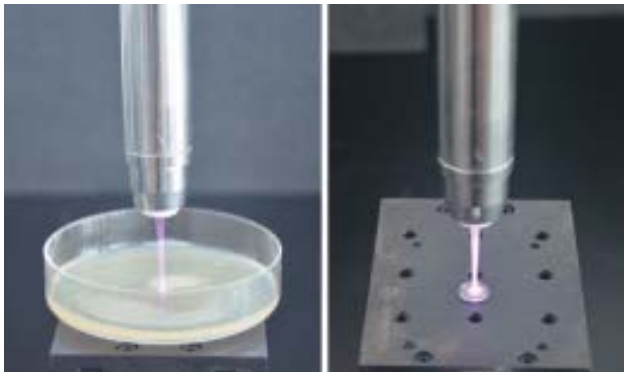

FIG. 3: Plasma treatment of agar plate (Φ 90 mm) and quartz plate (Φ 10 mm).

sodium chloride peptone buffer (pH 7.0), and 0.1 mL was then used to do HPCs. As a result, if 1 CFU was found on HPC agar plate, there were 20 survival bacteria on quartz surface. Each experiment was repeated for 3 times, and average results were then obtained.

III. RESULTS AND DISCUSSION

A. Typical Electrical Characteristics

Figure 4 presents typical pulsed-voltage/current waveforms and energy per pulse. As shown in Fig. 4(A), the peak voltage, peak current, and pulse width are 12 kV, 1.5 A, and 1.2 μs, respectively. By integrating voltage, current and time, the energy curve of single pulse can be obtained (Fig. 4B). The peak value is ~4.2 mJ, and the effective plasma energy is ~0.4 mJ. When the jet is operated at a frequency of 5–20 kHz, the corresponding

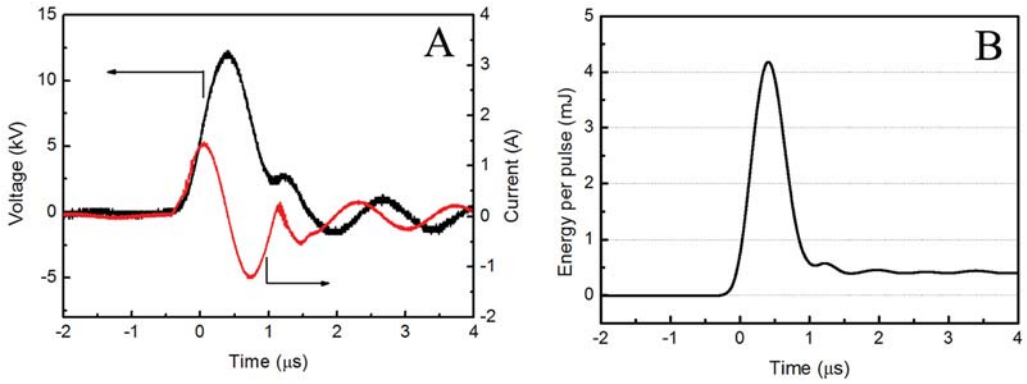

FIG. 4: Typical pulsed voltage/current waveforms (A) and energy per pulse (B).

plasma power is ~2–8 W. Because of the narrow pulse width and low power, the generated plasma jet is cold and can be directly applied on human skin (Fig. 1).

B. Generation of Helium Plasma Jet

Many factors can affect the formation of plasma jet such as pulsed voltage, operation frequency, and gas flow. Figure 5 shows the effect of peak voltage on the jet. The operational frequency is 15 kHz and the He flow rate is 4 L/min. When the peak voltage is <6 kV, no plasma jet is observed. However, if we observe the quartz tube, the He gas is ionized and luminous when the voltage is > 4 kV. A 5-mm-long plasma jet is obtained at a peak voltage of 7 kV. The length of plasma jet is significantly increased as increasing the peak voltage. The length of jet varies from 2.0 cm to 7.0 cm when the peak voltage is increased from 8 kV to 12 Kv (Fig. 5). Figure 6 gives the effect of operating frequency

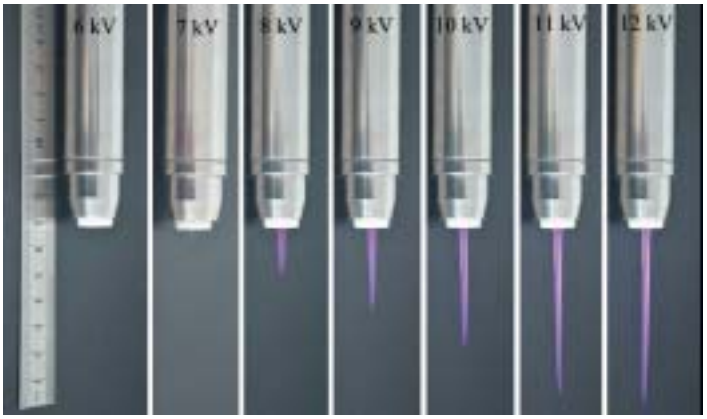

FIG. 5: Effect of peak voltage on helium plasma jet.

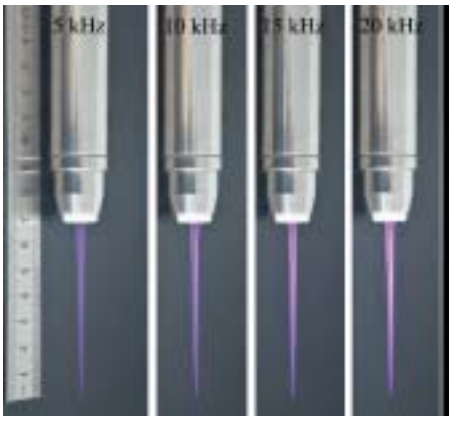

FIG. 6: Effect of operating frequency on helium plasma jet.

on plasma jet when it is operated at a peak voltage of 12 kV and an He flow rate of 4 L/min. When the operating frequency increases from 5 kHz to 20 kHz, the length of plasma jet remains almost the same, whereas the jet brightness is significantly enhanced.

Figure 7 illustrates the effect of gas flow rate on the He plasma jet when it is operated at a frequency of 15 kHz and a peak voltage of 12 kV. There is an optimal flow rate for the plasma jet. When the flow rate is 4 L/min, the jet has a maximal length of 7 cm. When the flow rate drops below this value, the jet is cone shaped and the length increases as the flow rate increases. The diameter of plasma jet is 4 mm at the nozzle exit, and gradually decreases as jet propagates. At the end of plasma jet, its diameter is <1 mm. When the flow rate is >4 L/min, the plasma jet is significantly disturbed by flow turbulence, and the jet length is dramatically reduced. Moreover, the plasma jet becomes more emanative. When the flow rate is >8 L/min, no significant influence on the plasma jet is observed, and the jet length is remains ~2 cm. This observation of the effect of gas flow agrees with other reports.[25, 26]

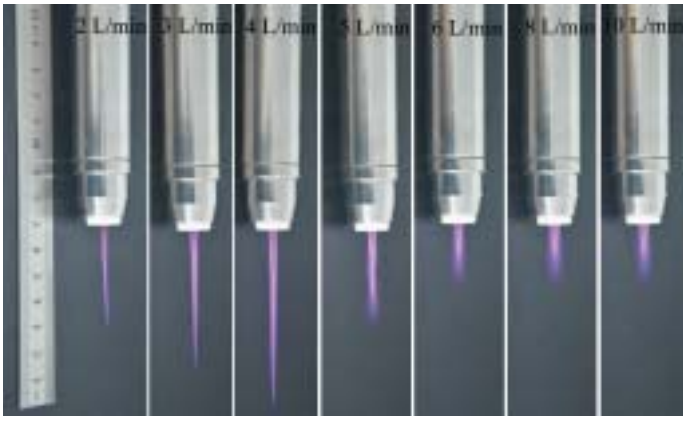

FIG. 7: Effect of gas flow rate on helium plasma jet.

C. Generation of Argon Plasma Jet

Compared with the He jet, the Ar plasma jet is difficult to generate. Figure 8 shows the effect of peak voltage on an Ar plasma jet when it is operated at a frequency of 15 kHz and an Ar flow rate of 4 L/min. When the peak voltage is no more than 7 kV, no plasma jet is observed. However, if we observe the quartz tube, the Ar gas is ionized and luminous at 7 kV. The voltage required for Ar gas ionization is higher than that for He gas. When the peak voltage is 8 kV, the Ar plasma jet starts to form, and the length is ~5 mm. Similarly, the length of the He jet increases as applied voltage increases. It increases from 0.5 cm to 3.0 cm when the peak voltage increases from 8 Kv to12 kV. For the present setup, the maximum length of the Ar plasma jet is <3 cm, and it is much shorter than that of the He plasma jet. Figure 9 gives the effect of operation frequency on the Ar plasma jet. The frequency has the same influence on the He jet as the Ar plasma jet.

FIG. 8: Effect of peak voltage on argon plasma jet.

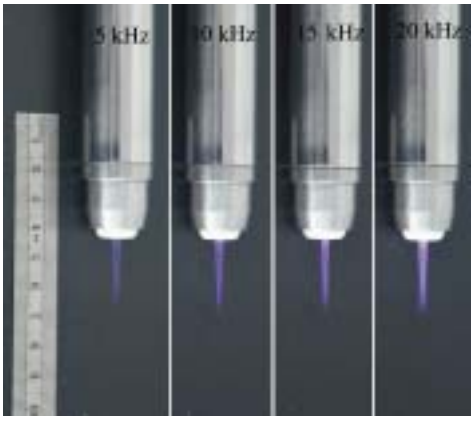

FIG. 9: Effect of operation frequency on argon plasma jet.

Figure 10 shows the effect of gas flow rate on the Ar plasma jet formation at an operating frequency of 15 kHz and a peak voltage of 12 kV. Similar to the He jet, there is an optimal flow rate to obtain a longest plasma jet. At a gas flow rate of 2 L/min, the length of the plasma jet is ~2.4 cm. The maximal length of 3 cm is obtained when the gas flow rate is increased to 4 L/min. When gas flow is 6 L/min, the length of plasma jet is 1.8 cm and become significantly shorter. No significant difference is observed when the flow rate is increased further, e.g., to 8 L/min and 10 L/min.

D. Emission Spectrum of Pulsed Plasma Jet

Figure 11 shows the emission spectrum of He and Ar plasma jets when they are operated at a peak voltage of 12 kV and a frequency of 15 kHz. An optical fiber was placed in front of plasma jet 3 cm away. During the measurement, signal of Ar was much stronger

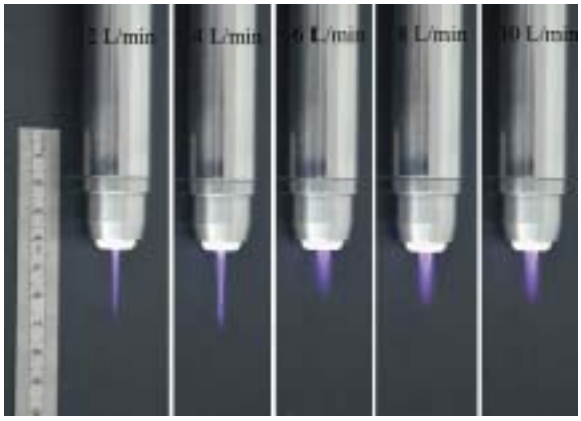

FIG. 10: Effect of gas flow rate on argon plasma jet.

than that of He. In fact, the integral times were set at 10 ms and 100 ms, respectively, for Ar and He, which means that the actual Ar emission was more than 10 times higher than that of He. However, the He plasma jet is brighter than that of Ar (Fig. 5 and Fig. 8). According to our elemental analysis, only 5 possible reactive He species can be induced by an He plasma jet: He I 706.52 [70], He I 587.60 [609], He I 667.82 [711], and He I 728.14 [48]. Moreover, there are more than 10 kinds of other reactive oxygen and nitrogen species. We suppose that He plasma lead to a second reaction and deionization when it meets atmospheric air. Thus, more visible spectral lines are generated that improve the visibility of the He plasma jet. For the Ar plasma jet, most of the spectral lines are reactive Argon species: Ar I 696.54 [28], Ar I 763.51 [214], Ar I 772.42 [314], and Ar I 826.45 [157]. Only one ROS and one RNS exist. Argon plasma reacts with ambient air with much more difficulty than He plasma, and this may be the reason the Ar plasma jet is shorter. The spectral lines of He plasma are mainly distributed from 300 nm to 800 nm, and those of Argon plasma are mainly focused between 700 nm and 1000 nm. This explains the different visibility characteristics of He and Ar plasma jets. Furthermore, no bactericidal UVC spectral line within 200–300 nm was observed in either the He or the Ar plasma jet.

E. Plasma Surface Disinfection

Disinfection is one of the most important applications for plasma medicine. Here, we present the preliminary results on the disinfection efficiency of this jet. Figure 12 shows the results of disinfection of *S. aureus* on an agar plate treated by an He plasma jet, where the pulsed voltage, operation frequency, and He flow rate are 12 kV, 20 kHz, and 4 L/min, respectively. The treatment distance, namely the distance from the nozzle exit to agar plate, is 4 cm (Fig. 3). After 0.5 min of treatment, a bactericidal spot of 5 mm was observed on agar plate. The diameter of bactericidal spot increased as treatment time increased. For the treatment times of 1.0 min, 1.5 min and 2 min, bactericidal spots 10

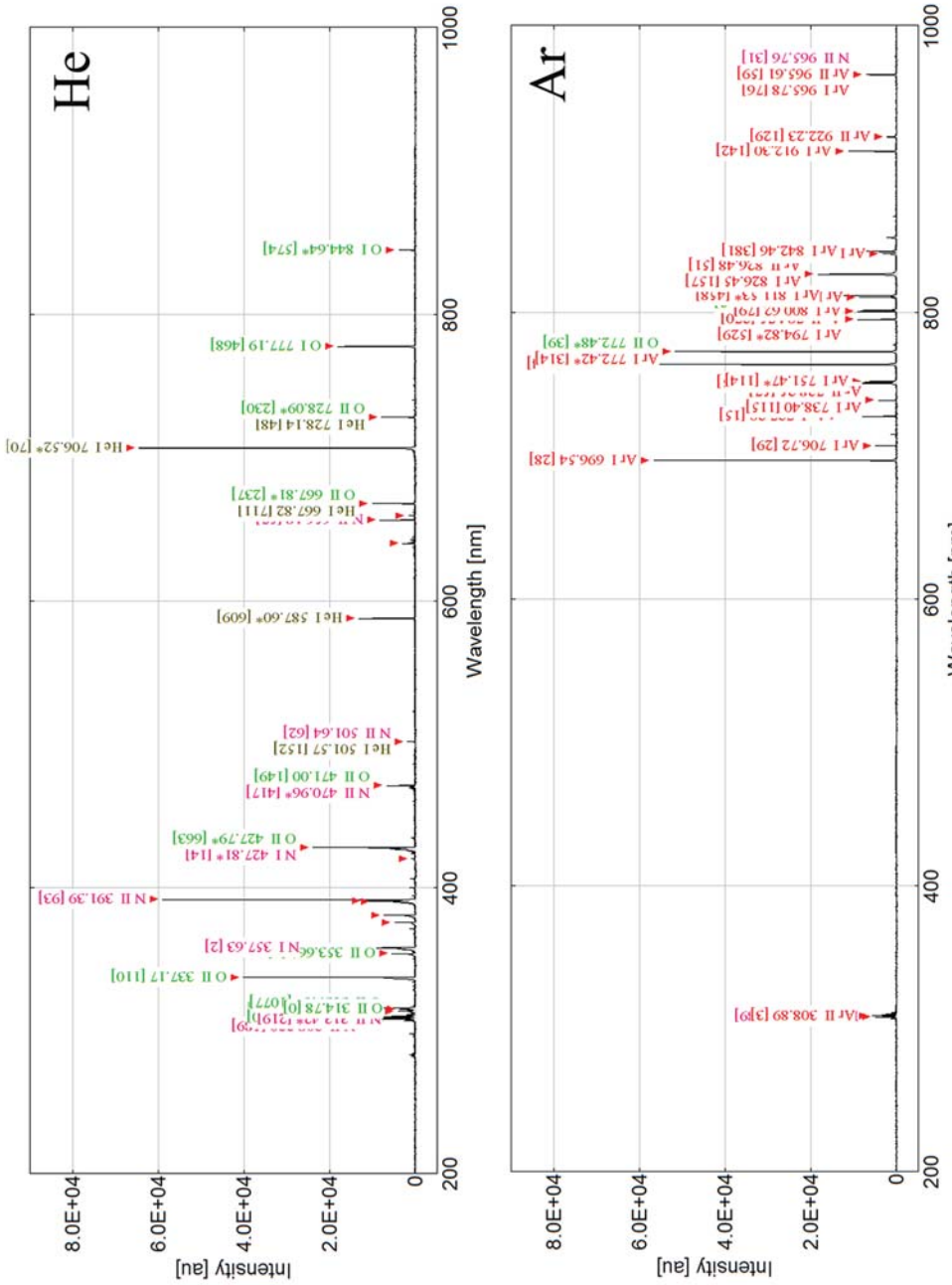

FIG. 11: Emission spectrum of helium (He) and argon (Ar) plasma jet.

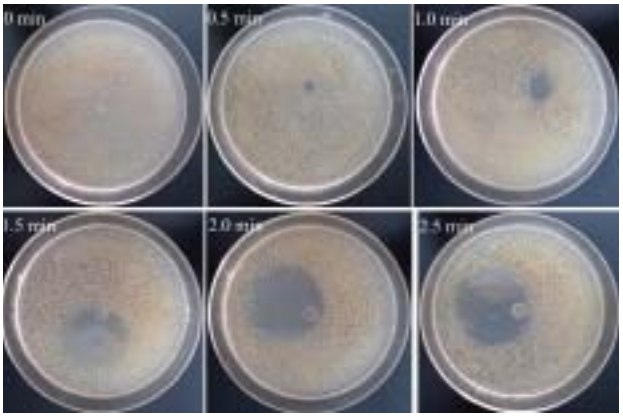

FIG. 12: Disinfection of *Staphylococcus aureus* on agar plate by helium plasma jet.

mm, 25 mm, and 35 mm in diameter were obtained. When treatment time was 2.5 min, no obviously increment of spot was observed. Thus, a 4-mm plasma jet can produce a bactericidal spot of up to 35 mm in 2 min.

Figure 13 shows the results of disinfection of *S. aureus* on an agar plate treated with an Ar plasma jet operated at a peak voltage of 12 kV, a frequency of 20 kHz, and a flow rate of 4 L/min. The treatment distance was 2 cm. After 0.5 min of treatment, a bactericidal spot of 10 mm in diameter was observed on the agar plate. The diameter of bactericidal spot increased as treatment time increased. For the treatment times of 1.0 min, 1.5 min, 2 min, and 2.5 min, the bactericidal spots of ~20 mm, ~30 mm, ~40 mm, and ~50 mm in diameter were obtained. To compare the disinfection efficiency on the *S. aureus* agar plate by He and Ar plasma jets, both flow rates were set to 6 L/min and treatment distance was 2 cm. The jet appearances are shown in Fig. 7 and Fig. 10. Peak voltage, pulsed frequency, and treatment time are 12 kV, 20 kHz, and 1.0 min. The results are shown in Fig. 14; the bactericidal spot diameter of He treatment is ~10 mm that of Ar treatment is 16 mm. Compared with the He plasma jet, the Argon plasma jet was more efficient for disinfection.

Figure 15 shows disinfection of *S. aureus* on a quartz plate by He and Ar plasma jets. The jets were operated at 12 kV, 20 kHz, at a flow rate of 6 L/min and a treatment distance of 2 cm (as in Fig. 14). The initial bacteria colony number was 8.0×10^4 CFU, and the bacteria density was ~1.0×10^5 CFU/cm^2. After 0.5 min of He plasma treatment, the bacteria number decreased to 6.2×10^3 CFU with a log reduction of 1.1. For Ar plasma, most of the bacteria had been eliminated after 0.5 min, with ~600 CFU residual and log reduction of 2.1. Furthermore, all bacteria were sterilized after 1 min of Ar plasma treatment. However, after He plasma treatment for 1 min, ~350 CFU remained. Approximately 1.5 min was required to realize sterilization with He plasma (Fig. 14). The Ar plasma jet performed more efficiently than the He plasma jet for disinfection.

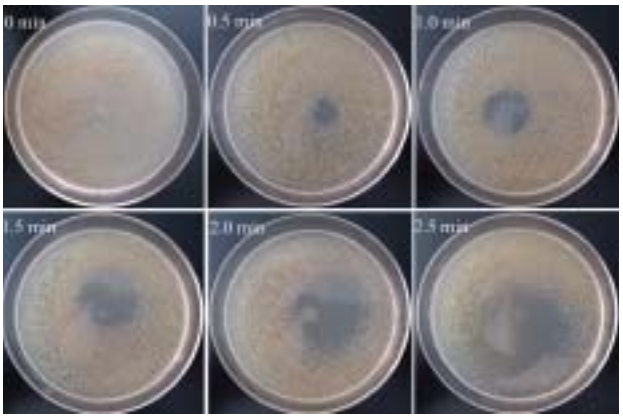

FIG. 13: Disinfection of *Staphylococcus aureus* on agar plate by argon plasma jet.

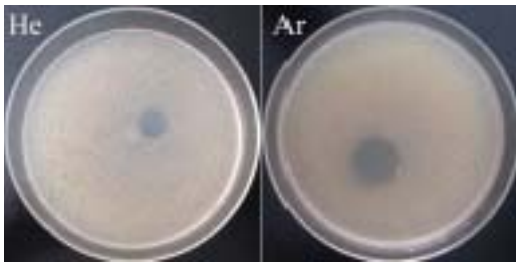

FIG. 14: Comparison of disinfection results on agar plate by helium and argon plasma jet.

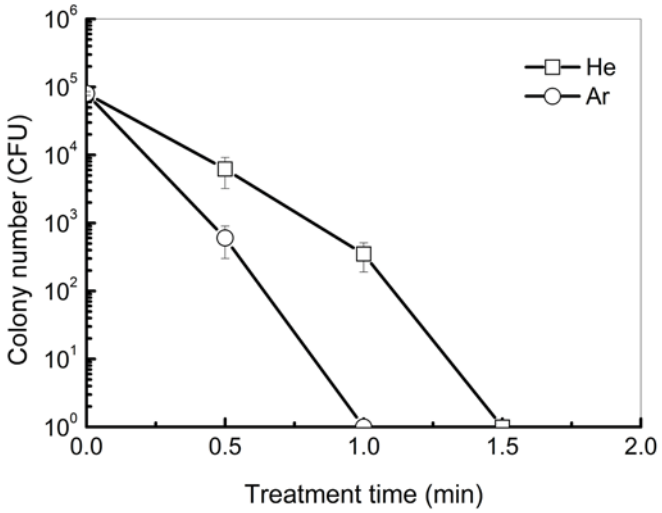

FIG. 15: Disinfection of *Staphylococcus aureus* on quartz plate by helium and argon plasma jet

IV. CONCLUSION

A microsecond-pulsed cold plasma jet device was developed. It consists of a microsecond-pulsed power source and a handheld jet gun. The gas flow rate was adjusted using a flow meter from 2 to 10 L/min. The average plasma power was <10 W. The He plasma jet was easier to generate than the Ar plasma jet. The maximum lengths for He and Ar plasma jets were 7 cm and 3 cm, respectively. Peak voltage and gas flow significantly affect plasma jet length, whereas the operation frequency only affects plasma brightness. Helium plasma is more visible than Ar plasma. When treating *S. aureus* on a 90-mm-diameter agar plate with the plasma jet, bactericidal spots up to 5 cm in diameter were observed after a 2.5-min treatment. For treating *S. aureus* on a 10-mm quartz plate, all bacteria were inactivated in 1.5 and 1 min by the He and Ar plasma jets, respectively. Argon plasma is more efficient than He for disinfection.

Disinfection is the basic medical function of cold plasma. For the present plasma jet device, more investigations are necessary to fully understand its characteristics including skin disinfection, wound healing, and other medical applications. Some other medical trials are also being undertaken using this cold plasma jet, for instance, treatment of onychomycosis on toenail and leukoderma on skin.

ACKNOWLEDGMENT

This research was funded by Science and Technology Program of Zhejiang Province (grant nos. 2015F10011 and 2014C33022), China.

REFERENCES

1. Daeschlein G, Scholz S, Ahmed R, Von Woedtke T, Haase H, Niggemeier M, Kindel E, Brandenburg R, Weltmann KD, Juenger M. Skin decontamination by low-temperature atmospheric pressure plasma jet and dielectric barrier discharge plasma. J Hosp Infect. 2012;81(3):177–83.
2. Kim HY, Kang SK, Park SM, Jung HY, Choi BH, Sim JY, Lee JK. Characterization and effects of Ar/Air microwave plasma on wound Healing. Plasma Process Polyme. 2015;12:1423–34.
3. Miyamoto K, Ikehara S, Takei H, Akimoto Y, Sakakita H, Ishikawa K, Ueda M, Ikeda J, Yamagishi M, Kim J, Yamaguchi T, Nakanishi T, Shimizu T, Shimizu N, Hori M, Ikehara Y. Red blood cell coagulation induced by low-temperature plasma treatment. Arch Biochem Biophys. 2016;605:95–101.
4. Graves D B. Reactive species from cold atmospheric plasma: implications for cancer therapy. Plasma Process Polyme. 2014;11(12):1120–7.
5. Cha S, Park YS. Plasma in dentistry. Clin Plasma Med. 2014;2:4–10.
6. Zhong S, Dong Y, Liu D, Xu D, Xiao SX, Chen HL, Kong MG. Surface air plasma-induced cell death and cytokine release of human keratinocytes in the context of psoriasis. Br J Dermatol. 2016;174:542–552.
7. Foster KW, Moy RL, Fincher EF. Advances in plasma skin regeneration. J Cosmet Dermatol. 2008;7(3):169–79.
8. Pierdzioch P, Hartwig S, Herbst SR, Raguse JD, Dommisch H, Abusirhan S, Wirtz HC, Hertel M, Paris S, Preissner S. Cold plasma: a novel approach to treat infected dentin—a combined ex vivo and in vitro study. Clin Oral Investig. 2016;20(9):2429–35.
9. Von Woedtke T, Metelmann HR, Weltmann KD. Clinical plasma medicine: state and perspectives of in vivo application of cold atmospheric plasma. Contribut Plasm Phys. 2014;54(2):104–17.

10. Ulrich C, Kluschke F, Patzelt A, Vandersee S, Czaika V, Richter H, Bob A, Von Hutten J, Painsi C, Huge R, Kramer A, Assadian O, Lademann J, Langeasschenfeldt B. Clinical use of cold atmospheric pressure argon plasma in chronic leg ulcers: a pilot study. J Wound Care. 2015;24(5):196–203.
11. Isbary G, Zimmermann J L, Shimizu T, Li YF, Morfill GE, Thomas HM, Steffes B, Heinlin J, Karrer S, Stolz W. Non-thermal plasma—more than five years of clinical experience. Clin Plasma Med. 2013;1(1):19–23.
12. Chen C, Liu D, Liu Z C, Yang AJ, Chen HL, Shama G, Kong MG. A model of plasma-biofilm and plasma-tissue interactions at ambient pressure. Plasma Chem Plasma P. 2014;34(3):403–441.
13. Graves D B. Oxy-nitroso shielding burst model of cold atmospheric plasma therapeutics. Clinical Plasma Medicine. 2014;2:38–49.
14. Bundscherer L, Wende K, Ottmuller K, Barton A, Schmidt A, Bekeschus S, Hasse S, Weltmann K, Kai Masur, Lindequist U. Impact of non-thermal plasma treatment on MAPK signaling pathways of human immune cell lines. Immunobiology. 2013;218:1248–55.
15. Miller V, Lin A, Fridman A. Why target immune cells for plasma treatment of cancer. Plasma Chem Plasma P. 2015;36:259–68.
16. Kilmer S, Semchyshyn N, Shah G, Fitzpatrick RE. A pilot study on the use of a plasma skin regeneration device (Portrait PSR3) in full facial rejuvenation procedures. Lasers Med Sci. 2007;22:101–9.
17. Isbary G, Stolz W, Shimizu T, Monetti R, Bunk W, Schmidt H, Morfill GE, Klampfl TG, Steffes B, Thomas HM, Heinlin J, Karrer S, Landthaler M, Zimmermann JL. Cold atmospheric argon plasma treatment may accelerate wound healing in chronic wounds: results of an open retrospective randomized controlled study *in vivo*. Clin Plasma Med. 2013;1:25–30.
18. Bekeschus S, Schmidt A, Weltmann KD, Von Woedtke T. The plasma jet kINPen—a powerful tool for wound healing. Clin Plasma Med. 2016;4:19–28.
19. Simoncelli E, Barbieri D, Laurita R, Liguori A, Stancampiano A, Viola L, Tonini R, Gherardi M, Colombo V. Preliminary investigation of the antibacterial efficacy of a handheld plasma gun source for endodontic procedures. Clin Plasma Med. 2015;3:77–86.
20. Wu S, Cao Y, Lu X. The state of the art of applications of atmospheric-pressure nonequilibrium plasma jets in dentistry. IEEE Trans Plasma Sci. 2016;44(2):134–51.
21. Morfill G E, Shimizu T, Steffes B, Schmidt H. Nosocomial infections—a new approach towards preventive medicine using plasmas. New J Phys. 2009;11:115019(10pp).
22. Li Y F, Taylor D, Zimmermann JL, Bunk W, Monetti R, Isbary G, Boxhammer V, Schmidt H, Shimizu T, Thomas HM, Morfill GE. In vivo skin treatment using two portable plasma devices: comparison of a direct and an indirect cold atmospheric plasma treatment. Clin Plasma Med. 2013;1:35–9.
23. Pei X, Lu X, Liu J, Liu D, Yang YJ, Ostrikov K, Chu PK, Pan Y. Inactivation of a 25.5 μm Enterococcus faecalis biofilm by a room-temperature, battery-operated, handheld air plasma jet. J Phys D Appl Phys. 2012;45:165205 (5pp).
24. Robert E, Vandamme M, Brulle L, Lerondel S, Pape AL, Sarron V, Ries D, Darny T, Dozias S, Collet G, Kieda C, Pouvesle JM. Perspectives of endoscopic plasma applications. Clinical Plasma Medicine. 2013;1:8–16.
25. Li Q, Li JT, Zhu WC, Zhu XM, Pu YK. Effects of gas flow rate on the length of atmospheric pressure nonequilibrium plasma jets. Appl Phys Lett. 2009;95:141502(3pp).
26. Xiong Q, Lu X F, Ostrikov K, Xiong Z, Xian YB, Zhou FB, Zou CL, Hu J, Gong W, Jiang ZY. Length control of He atmospheric plasma jet plumes: effects of discharge parameters and ambient air. Phys Plasmas. 2009;106:013308 (7pp).